Endocardium is necessary for cardiomyocyte movement during heart tube assembly

Development 134, 2379-2386 (2007) doi:10.1242/dev.02857

Endocardium is necessary for cardiomyocyte movement during heart tube assembly

Nathalia Glickman Holtzman[1,2], Jeffrey J. Schoenebeck[1], Huai-Jen Tsai[3] and Deborah Yelon[1,*]

Embryonic heart formation requires the union of bilateral populations of cardiomyocytes and their reorganization into a simple tube. Little is known about the morphogenetic mechanisms that coordinate assembly of the heart tube and determine its dimensions. Using time-lapse confocal microscopy to track individual cardiomyocyte movements in the zebrafish embryo, we identify two morphologically and genetically separable phases of cell movement that coordinate heart tube assembly. First, all cardiomyocytes undergo coherent medial movement. Next, peripherally located cardiomyocytes change their direction of movement, angling toward the endocardial precursors and thereby establishing the initial circumference of the nascent heart tube. These two phases of cardiomyocyte behavior are independently regulated. Furthermore, we find that myocardial-endocardial interactions influence the second phase by regulating the induction, direction and duration of cardiomyocyte movement. Thus, the endocardium plays a crucial early role in cardiac morphogenesis, organizing cardiomyocytes into a configuration appropriate for heart tube assembly. Together, our data reveal a dynamic cellular mechanism by which tissue interactions establish organ architecture.

KEY WORDS: Endocardium, Myocardium, Zebrafish, *cloche*, *miles apart* (*edg5*), Morphogenesis

INTRODUCTION

Organogenesis requires the precise arrangement of numerous cells into a specific three-dimensional architecture that is essential for effective organ function. Cardiogenesis, for example, involves a series of morphogenetic steps that must be carefully orchestrated in order to insure the proper dimensions of the heart tube. In all vertebrate embryos, heart tube assembly begins with the medial movement of bilateral groups of cardiomyocytes (Glickman and Yelon, 2002; Harvey, 2002; Moorman and Christoffels, 2003). Once they reach the embryonic midline, the bilateral populations merge through a process called cardiac fusion. Cardiac fusion produces an intermediate structure, referred to as a cardiac crescent in amniotes (Harvey, 2002; Moorman and Christoffels, 2003) and a cardiac cone in zebrafish (Glickman and Yelon, 2002), that gradually transforms into a primitive heart tube. This simple cylinder immediately becomes responsible for driving embryonic circulation; therefore, the precise coordination of heart tube assembly has significant consequences for embryonic physiology.

Previous studies of heart tube assembly in the zebrafish embryo have provided an overview of this dynamic process. Cardiac fusion initiates with contacts between posterior subsets of contralateral cells, followed by interactions between anterior subsets of contralateral cells (Glickman and Yelon, 2002; Yelon et al., 1999) (Fig. 1A). These connections create a ring of cardiomyocytes surrounding the centrally located precursors of the vascular endocardium (Stainier et al., 1993; Trinh and Stainier, 2004) (Fig. 1A). Next, the myocardial ring, which is also called the cardiac cone, converts into a tube (Glickman and Yelon, 2002; Stainier et al., 1993; Yelon et al., 1999). Through gradual extension of the length of its axis, the once shallow cone becomes an elongated cylinder, and the inner and outer circumferences of the cone become the arterial and venous apertures of the nascent heart tube (Glickman and Yelon, 2002; Stainier et al., 1993; Yelon et al., 1999). At the same time, the endocardial precursors spread out to create the endothelial lining of the myocardial cylinder (Stainier et al., 1993). Thus, the cardiac cone provides an essential foundation for the dimensions and composition of the zebrafish heart tube.

Despite the importance of creating a strong foundation for heart tube formation, the morphogenetic mechanisms that regulate cardiomyocyte behavior during this process remain relatively undefined. Work in multiple model organisms has indicated that interactions between the myocardium and neighboring gut endoderm are crucial for the recruitment of cardiomyocytes toward the embryonic midline (e.g. Dickmeis et al., 2001; Kikuchi et al., 2001; Li et al., 2004; Narita et al., 1997). Medial recruitment also appears to require the organization of cardiomyocytes into polarized epithelia. During cardiac fusion, cardiomyocytes begin to form the junctional complexes typical of epithelia and exhibit molecular characteristics of apicobasal polarity (Trinh and Stainier, 2004). Mutations that interfere with epithelialization, such as *natter* (also known as *fibronectin 1*), prevent cardiomyocytes from moving properly toward the midline (Trinh and Stainier, 2004). However, it is not clear whether the proximity of the contralateral myocardial populations at the midline is sufficient to coordinate their integration into a heart tube. Does tube construction simply result from a continuation of the initial medial movement of cardiomyocytes, or does it require a distinct mode of cell behavior subject to independent regulation?

To distinguish between these models, we have used time-lapse imaging to resolve the direction, rate and organization of individual cardiomyocyte movements during cardiac fusion in wild-type and mutant zebrafish embryos. Our data indicate that two morphologically and genetically separable phases of cardiomyocyte movement underlie cardiac fusion: a first phase that recruits cells toward the midline and a second phase that creates the morphology of the cardiac cone. Additionally, we find that cardiomyocyte

[1]Developmental Genetics Program and Department of Cell Biology, Skirball Institute of Biomolecular Medicine, New York University School of Medicine, New York, NY 10016, USA. [2]Department of Biology, Queens College, The City University of New York, Flushing, NY 11367, USA. [3]Institute of Molecular and Cellular Biology, National Taiwan University, Taipei, Taiwan.

*Author for correspondence (e-mail: yelon@saturn.med.nyu.edu)

Accepted 28 March 2007

movement during the second phase is regulated by the presence of the endocardium, thereby revealing a previously unappreciated role for myocardial-endocardial interactions during heart tube assembly.

MATERIALS AND METHODS

Embryo collection and preparation

Wild-type fish and heterozygotes for the mutations *clo*^{s5} and *mil*^{te273} (Chen et al., 1996; Qian et al., 2005) carrying *Tg(cmlc2:egfp)* (Huang et al., 2003) were mated to generate experimental embryos. Embryos were screened for robust *egfp* expression using a Zeiss M2Bio microscope. For *mil* mutants, the genotype was assessed prior to time-lapse imaging: these mutants exhibit a clear cardia bifida phenotype at the 18-somite stage (Yelon et al., 1999). Selected embryos were mounted in a drop of 3% methylcellulose within a larger drop of 2% low-melting point agarose in embryo medium. Mounting slides were constructed by placing a single layer of electrical tape on a standard microscope slide and cutting a small square out of the center to create a well. Embryos were oriented to permit a dorsal view of the heart fields, using the tip of the notochord as a guide. Finally, a drop of embryo medium with tricaine was placed on top of each agar-mounted embryo.

Data collection and processing

Embryos were maintained at 28.5°C during data collection, using an upright Zeiss LSM510 confocal microscope equipped with a heated stage, a 25× Plan-Neofluor multi-immersion objective and LSM510 software. In order to generate 3D reconstructions, 30-40 focal planes were collected at intervals of 1.5-2.5 μm, a distance sufficient to accommodate sample movement during the course of the time-lapse. Images were collected at 2-3 minute intervals. Typically, time-lapses began around the 15- to 18-somite stage and ended at the completion of fusion, around the 20- to 21-somite stage. Time of initial imaging was often dependent upon GFP intensity, which varies at early stages. After imaging, embryos were coaxed from their mounting agar and transferred to fresh embryo medium. Embryonic stage was determined both before and after mounting; manipulation and imaging did not delay development. Additionally, embryonic health and genotype were assessed at 24 hours post-fertilization (hpf). Only data collected from embryos that appeared completely normal at 24 hpf were analyzed.

For 4D analysis, LSM510 databases were imported into a Volocity (Improvision) library. An image sequence composed of a linear array of 3D-rendered time points was then generated for each data set. As appropriate, image appearance (brightness, contrast, opacity) was modified to optimize visualization of cells of interest. Optimization of image appearance was a key step: GFP intensity varies widely among individual cardiomyocytes and increases over time, so resolution of each cell required different adjustments of image settings. Image settings shown in Figs 1-4 allow resolution of many, but not all, tracked cells. Images were exported as QTmov files for visualization of a time-lapse from a preset view.

Cell tracking and analysis

Examination of high-resolution confocal images indicated that the myocardium is a relatively flat sheet of cells, approximately 8 μm thick, from the 15- to 20-somite stages (N.G.H. and D.Y., unpublished). During these stages, most cardiomyocyte movement is along the *x* (mediolateral) and *y* (anteroposterior) axes, rather than along the *z* (dorsoventral) axis. The *z*-axis displacement of tracked cardiomyocytes did not exceed one cell diameter over the course of our time-lapses. Therefore, when tracking cardiomyocyte movements, we treated the myocardium as a 2D tissue and focused on tracking the *x* and *y* coordinates of the center of each cell. At time points following our window of analysis, we have observed significant dorsal cardiomyocyte movements as the cardiac cone extends into a tube (N.G.H. and D.Y., unpublished). These dorsal movements are consistent with prior histological observations (Stainier et al., 1993; Trinh and Stainier, 2004), although we have not observed lateral displacement of dorsal cardiomyocytes as suggested by Trinh and Stainier (Trinh and Stainier, 2004).

For each time-lapse, we examined all *z*-stack images and tracked as many cells as were resolvable in any focal plane throughout the entire period of imaging. Figs 1-4 show reconstructed projections of *z*-stacks and include a representative subset of tracks from the time-lapses depicted. To track a cell, we selected a pixel at its visual center at each time point, modifying the image intensity as necessary, and recorded each pixel's coordinates using Volocity. Each series of cell locations was then converted to a track using Volocity's 'manual track' function. This function automatically generates a measurement file that includes the distance traveled, velocity and a series of *xy* positions for each cell. These files were exported into Microsoft Excel for further analysis, including calculation of net direction of movement. To visually depict cell tracks (as in Fig. 1E-I, Fig. 2C-E and Fig. 3C,D) we generated lines connecting each series of cell locations, added arrowheads to indicate the direction of movement, and overlaid these tracks on processed images of individual time points. As a control for accuracy of tracking, all of the cells in one wild-type embryo were tracked twice. The two sets of distances, velocities and directions of movement did not vary by more than 5%.

For quantitative analysis of the net direction of movement for each tracked cell, we calculated the percentage of the *y*-axis displacement relative to the *x*-axis displacement in radians, using the formula: $(\Delta y/\Delta x)\times 100$. This can also be expressed as an angle (°) using the formula: $\text{atan}(\Delta y/\Delta x)\times 57.295$. The resulting value reflects the cell's degree of displacement along the anterior-posterior axis: a value of 0° corresponds to direct medial movement, and a value of 90° corresponds to direct anterior or posterior movement. Examination of the degree of displacement of wild-type cardiomyocytes during the first phase of cardiac fusion demonstrated that more than 80% of these cells were displaced by less then 30° (Fig. 1J). We therefore defined 'medial movement' as a displacement of less than 30° and 'angular movement' as a displacement of greater than 30°. Some tracked cells exhibited little movement: we defined 'no net displacement' as movement of less than 10% of a cell diameter over the course of a 20-minute period (as in Fig. 1I). Additionally, we defined 'no net directed movement' as failure to move beyond a cell diameter from the starting position over the course of a time-lapse lasting at least 90 minutes (as in Fig. 4C,D).

To compare regional differences in the patterns of cardiomyocyte movement, we divided the bilateral cardiomyocyte populations into three regions: anterior, central and posterior. In wild-type embryos, we defined regions retrospectively, based on the positions of individual medial cardiomyocytes at the completion of cardiac fusion (Fig. 1M). Cells located at the anterior or posterior interfaces between contralateral populations were considered to be in anterior or posterior regions, respectively. Cells located between these areas were considered to be in the central region. In *clo*, *mil* and *mil;clo* mutant embryos, we defined regions differently, as cardiac cone morphology is aberrant. In these cases, we divided populations into equivalent thirds along the anterior-posterior axis, based on the number of cells present at the medial edge of the population at the beginning of the time-lapse (Fig. 2G and Fig. 3F).

In situ hybridization

Single-color whole-mount in situ hybridization for *cmlc2* and *flk1* was performed according to a standard protocol (Liao et al., 1997; Yelon et al., 1999). Two-color fluorescent whole-mount in situ hybridization was conducted according to a protocol that will be reported separately (J.J.S., B. R. Keegan and D.Y., unpublished). Riboprobes for *cmlc2* and *fli1a* (Thompson et al., 1998) were labeled with dinitrophenol (Mirus) and digoxygenin (Roche) haptens and detected by deposition of Cy3 and fluorescein tyramides (PerkinElmer), respectively.

RESULTS

Tracking cardiomyocyte movement during heart tube assembly

To examine dynamic cell movements during heart tube assembly, we took advantage of a reporter transgene, *Tg(cmlc2:egfp)*, that drives *egfp* expression in cardiomyocytes (Huang et al., 2003). *Tg(cmlc2:egfp)* expression mimics endogenous *cardiac myosin light chain 2* (*cmlc2*; *myl7* – ZFIN) expression, beginning before cardiomyocytes approach the embryonic midline and continuing throughout development (Huang et al., 2003; Yelon et al., 1999) (Fig. 1B-D). We visualized cell movements over time by collecting confocal *z*-stacks at 2-minute intervals and rendering a three-dimensional time-lapse. To quantify patterns of cell behavior, we

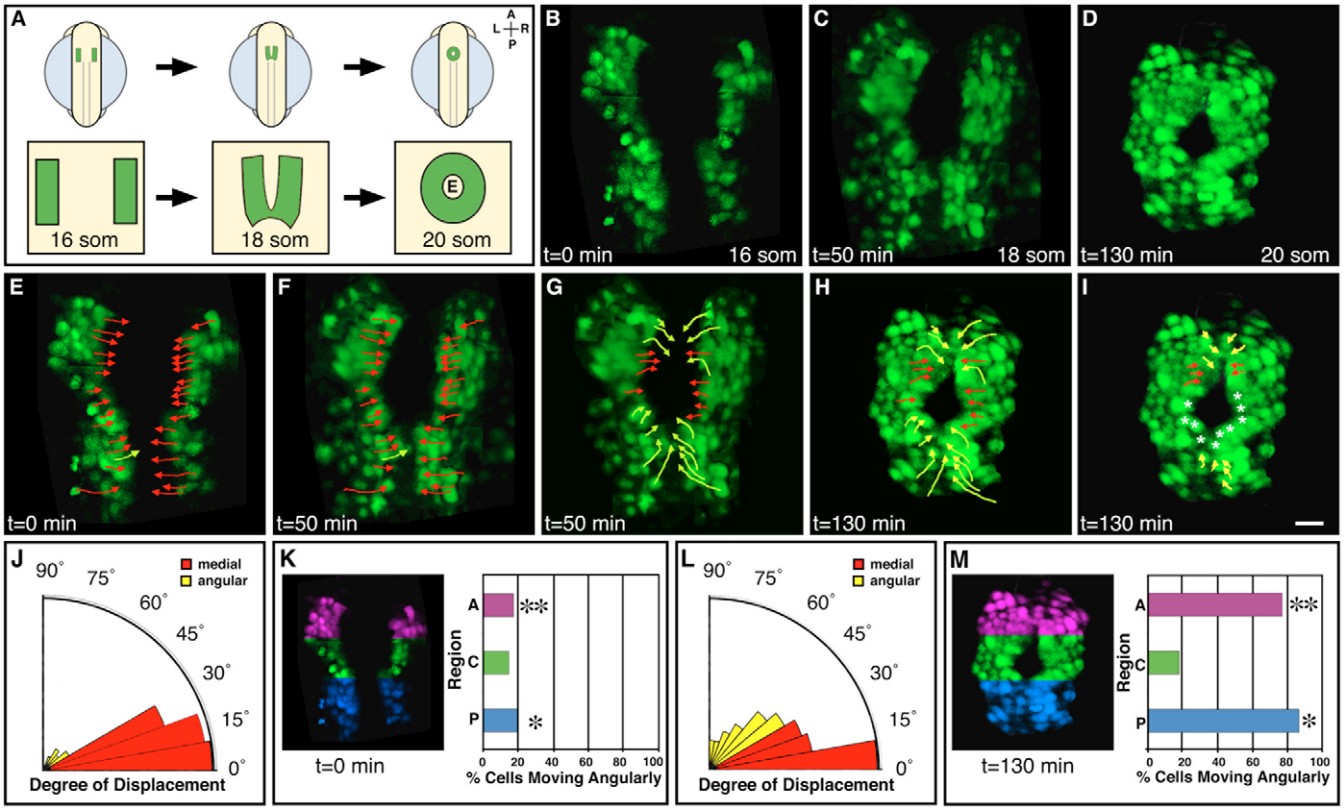

Fig. 1. Tracking wild-type cardiomyocytes reveals two morphologically distinct phases of cell behavior during cardiac fusion. (**A**) Schematic of cardiac fusion in the zebrafish embryo. Dorsal views; locations of cardiomyocyte populations shown in green; location of endocardium at the 20-somite stage indicated with an E. (**B-D**) Selected images from a time-lapse of cardiac fusion in a typical wild-type embryo expressing *Tg(cmlc2:egfp)* (see Movie 1 in the supplementary material), exhibiting cardiac morphology at the (B) 16-somite, (C) 18-somite and (D) 20-somite stages. Dorsal views, anterior to the top. (**E-I**) Paths traveled by individual cardiomyocytes during (E,F) the initial 50 minutes, (G,H) the final 80 minutes and (I) the final 20 minutes of fusion. Tracks displayed represent a subset of the tracked cells in this time-lapse. Each arrow extends from a cell's starting position to its ending position. Red arrows, medial movement; yellow arrows, angular movement; asterisks, cells exhibiting no net displacement over the elapsed time. Cardiac fusion begins with a phase of coherent medial movement (E,F), followed by a transition to angular movement in anterior and posterior regions (G,H). Scale bar: in I, 20 μm for B-I. (**J-M**) Quantitative analysis of the direction of cardiomyocyte movement. (J,L) Radial bar graphs depict degree of cardiomyocyte displacement during the first (J) and second (L) phases. For all tracked wild-type cardiomyocytes, net displacement along the anterior-posterior axis was calculated relative to a directly medial path (0° displacement). Grouping the data in 10° increments, the length of each radial bar reflects the percentage of cells exhibiting each degree of displacement. Red bars are classified as medial movement, and yellow bars are classified as angular movement. Significantly more cells exhibit angular movement during the second phase than during the first phase (52% versus 17%; *t*-test, $P<0.01$). (K,M) Location of cardiomyocytes moving angularly during first (K) and second (M) phases. Colors overlaid on *egfp* expression reflect anterior (purple), central (green) and posterior (blue) regions. Most of the cells exhibiting angular movement are located in anterior or posterior regions. In these regions, the percentage of cells moving angularly during the second phase is significantly greater than that observed during the first phase (*, posterior: 86% versus 20%; **, anterior: 77% versus 17%; *t*-test, $P<0.01$ for both regions). See Materials and methods for details of time-lapse analysis and Table 1 for additional data.

measured the displacement of individual cells between time points, creating a track representative of each cell's movement over time (detailed imaging and tracking protocols are provided in the Materials and methods). Using this strategy, we resolved the direction, rate and organization of individual cardiomyocyte movements throughout the process of cardiac fusion. Although we focused our analysis on cells at the medial edge of each cardiomyocyte population, we also found that lateral cells exhibit comparable patterns of movement (data not shown).

Coherent medial movement brings cardiomyocytes to the midline

Previous gene expression studies and fate-map analyses in zebrafish, chick and mouse embryos have suggested that cardiomyocytes advance toward the midline in an orderly fashion (Dehaan, 1963; Keegan et al., 2004; Lyons et al., 1995; O'Brien et al., 1993; Stalsberg and DeHaan, 1969; Yelon et al., 1999). In accordance with these previous studies, our time-lapse examination of wild-type embryos demonstrated that cardiac fusion begins with a phase of coherent medial movement that brings the cardiomyocytes into position for the initiation of cardiac cone formation (Fig. 1B,C,E,F and see Movie 1 in the supplementary material). All cardiomyocytes exhibited similar patterns of behavior, following relatively parallel paths of similar length with general maintenance of neighbor relationships (Fig. 1E,F). Examination of cell tracks revealed that most cardiomyocytes move directly toward the midline, exhibiting an angular displacement of less than 30° along the anterior-posterior axis (Fig. 1J and Table 1). We classify this behavior as 'medial movement' (red arrows/bars), in contrast to 'angular movement' (yellow arrows/bars), which we define as an angular displacement of greater than 30° (Fig. 1E,F,J). Overall, the observed coherence

Table 1. Direction of cardiomyocyte movement during cardiac fusion

		Medial movement		Angular movement		No net movement
Genotype	Region	*n*	Angle	*n*	Angle	*n*
Wild type	A	19	15°±2°	4	61°±9°	0
Phase 1	C	46	12°±1°	8	41°±4°	0
5 embryos	P	28	15°±3°	7	50°±4°	0
Wild type	A	6	16°±2°	20	49°±4°	0
Phase 2	C	45	12°±1°	10	49°±4°	0
5 embryos	P	5	13°±2°	32	57°±4°	0
clo	A	24	7°±1°	3	44°±3°	0
4 embryos	C	19	9°±1°	7	46°±7°	0
	P	28	11°±1°	19	68°±3°	0
mil	A	1	15°	13	65°±4°	0
2 embryos	C	0	na	2	55°±7°	16
(4 fields)	P	6	25°±3°	16	62°±6°	0
mil;clo	A	0	na	0	na	21
2 embryos	C	0	na	0	na	24
(4 fields)	P	0	na	0	na	25

na, not applicable.
For each genotype, tracked cells are classified by region (A, anterior; C, central; or P, posterior) and by net direction of movement (medial, angular, or no net directed movement). Wild-type data are further subdivided to demonstrate differences in cardiomyocyte behavior during the first and second phases of cardiac fusion. The total number (*n*) of tracked cardiomyocytes in each category is indicated, as is the mean angle of movement±s.e.

of cardiomyocyte movement is consistent with the status of the migrating myocardium as a maturing, polarized epithelium (Trinh and Stainier, 2004).

Regionally restricted angular movement facilitates cone formation

We observed a striking transition in cardiomyocyte behavior once the contralateral populations initiate contact at the midline. Specifically, we found that many cardiomyocytes switch from medial movement to angular movement (Fig. 1C,D,G,H,L, Table 1 and see Movie 1 in the supplementary material). Most of the cells exhibiting angular movement are located in the anterior or posterior region of each heart field (angular movement observed in 20 of 26 anterior cells and 32 of 37 posterior cells, Fig. 1M and Table 1), with anterior cells angling toward the posterior and posterior cells angling toward the anterior (Fig. 1G,H). By contrast, cells located in the central region of each field tended to continue to move medially (medial movement observed in 45 of 55 central cells, Fig. 1M and Table 1). This pattern of behavior is a significant departure from the first phase of cardiac fusion, during which very few cardiomyocytes in anterior or posterior regions exhibit angular movement (Fig. 1K,M and Table 1). Thus, these regional changes in direction of movement distinguish a second phase of cardiac fusion.

As a consequence of regional transitions to angular movement, the bilateral populations of cardiomyocytes formed mirror-image arcs, ultimately encircling the endocardial precursors and creating the cardiac cone (Fig. 1C,D,G,H). Regional differences in the duration of movement also contribute to arc formation. Although all cardiomyocytes moved at comparable rates during the second phase of cardiac fusion (0.36±0.03 μm/minute), cells in central regions tended to stop moving earlier than cells in anterior or posterior regions. Examination of cell movements during the final 20 minutes of cone formation (20 minutes before the 20-somite stage, Fig. 1I) revealed that most centrally located cells exhibit no net displacement during this interval [64% (35 of 55) of cells examined; white asterisks]. By contrast, most cells in anterior and posterior regions continued moving during this time interval, with only 33% (21 of 63) of these cells coming to a halt. Together, our data indicate that regionally restricted transitions in the direction and duration of cardiomyocyte movement facilitate cardiac cone formation.

No angular movement in the absence of endocardium

Our time-lapse analyses in wild-type embryos indicated that cardiac fusion involves two morphologically distinct phases of cell behavior. We hypothesized that these two phases could represent separately regulated morphogenetic processes, with endoderm-derived cues driving the initial medial movement (Alexander et al., 1999; Dickmeis et al., 2001; Kikuchi et al., 2001; Kupperman et al., 2000) and independent cues triggering the transition from medial to angular movement. Previous studies have suggested that the endocardial precursors cluster at the future center of the cardiac cone (Stainier et al., 1993; Trinh and Stainier, 2004). To test whether the endocardium influences the redirection of anterior and posterior cardiomyocytes toward a central point, we tracked cardiomyocyte movements in *cloche* (*clo*) mutant embryos (Stainier et al., 1995). Although the identity of the *clo* gene has not yet been reported, prior analyses have established that *clo* is required cell-autonomously for formation of endothelial precursors, and *clo* mutants therefore exhibit a general loss of endothelium, including the endocardium (Liao et al., 1997; Stainier et al., 1995).

Examination of *clo* mutants demonstrated that cardiac fusion begins normally in the absence of endocardium. The medial direction of movement exhibited by *clo* mutant cardiomyocytes (Fig. 2A-D and see Movie 2 in the supplementary material) resembled the initial behavior of wild-type cardiomyocytes (Fig. 1E,F). Additionally, the mean rate of *clo* mutant cardiomyocyte movement (0.62±0.12 μm/minute) was similar to the mean rate observed during the first phase of wild-type cardiac fusion (0.68±0.04 μm/minute). However, in contrast to wild-type behavior, *clo* mutant cardiomyocytes failed to make a transition to angular movement (Fig. 2C,D,F,G,H and Table 1). Instead, anterior and posterior *clo* mutant cardiomyocytes continued to move medially throughout cardiac fusion. Additionally, central cardiomyocytes in *clo* mutants remained in motion over a longer duration than their wild-type counterparts (compare Fig. 2E with Fig. 1I). During the last 20 minutes of cone formation, only 31% (10 of 26) of the centrally located cells tracked in *clo* mutant embryos came to a halt. Together, these abnormal movement patterns result in the formation of a dysmorphic cardiac cone (Fig. 2B). Thus, the *clo* mutant phenotype suggests that the endocardium exerts significant influence on the direction and duration of cardiomyocyte movement during the second phase of cardiac fusion. Subsequently, heart tube extension proceeds slowly and aberrantly in *clo* mutants, such that the misshapen cardiac cone transforms into an abnormally short and wide tube (Fig. 2I,J). The aberrant dimensions of the *clo* mutant cardiac cone might be directly responsible for the dimensions of the *clo* mutant heart tube. However, it is also possible that the morphology of the *clo* mutant heart tube reflects a separate role of the endocardium in regulating heart tube extension.

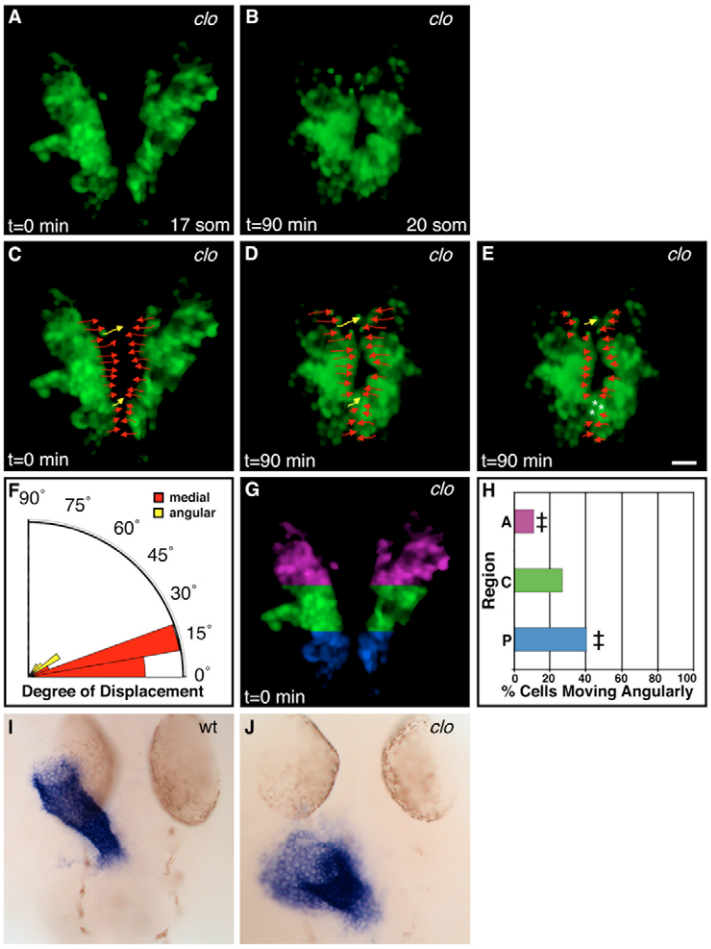

Fig. 2. No angular movement in the absence of endocardium. (**A**,**B**) Selected images from a time-lapse of cardiac fusion in a typical *clo* mutant zebrafish embryo expressing *Tg(cmlc2:egfp)* (see Movie 2 in the supplementary material), exhibiting cardiac morphology at the (A) 17-somite and (B) 20-somite stages. Dorsal views, anterior to the top. (**C-E**) Paths traveled during the (C,D) entire 90 minutes and (E) final 20 minutes of fusion (arrows and asterisks as described for Fig. 1). Tracks displayed represent a subset of the tracked cells in this time-lapse. In *clo* mutants, cardiomyocytes exhibit medial movement throughout the duration of cardiac fusion. Scale bar: in E, 20 μm for A-E. (**F**) Radial bar graph (see Fig. 1J,L) depicting degree of displacement for all tracked *clo* mutant cardiomyocytes. Few cells exhibit angular movement, resembling the pattern of cell behavior observed during the first phase of wild-type fusion (see Fig. 1J). (**G**,**H**) Location of cardiomyocytes moving angularly in *clo* mutants. In anterior (purple) and posterior (blue) regions (‡), the percentage of cells moving angularly is significantly reduced (*t*-test, $P<0.01$) compared with that observed during the second phase of wild-type fusion (see Fig. 1M). See Table 1 for additional data. (**I**,**J**) In situ hybridization depicts *cmlc2* expression in wild-type (I) and *clo* mutant (J) embryos at 28 hpf. Dorsal views, anterior to the top; both images shown at the same magnification. Elongation of the heart tube is delayed and aberrant in *clo* mutant embryos.

Angular movement in the absence of prior medial movement

The aberrant patterns of cell behavior in *clo* mutants suggest that the endocardium might actively guide the direction of cardiomyocyte movement. Alternatively, the endocardium might play a more passive role in shaping the cardiac cone, perhaps by creating an obstacle for the moving cardiomyocytes. In this scenario, the central location of the endocardium, together with the intracellular junctions connecting the myocardial epithelium (Trinh and Stainier, 2004), could create physical constraints for the medially migrating cardiomyocytes, resulting in the conversion of medial movement into angular movement at the anterior and posterior ends of each heart field. To test whether the transition to angular movement requires an initial phase of medial movement, we tracked cardiomyocyte movement in mutants exhibiting cardia bifida, a phenotype in which the heart fields do not move toward the midline and instead form two lateral hearts. Zebrafish mutations that disrupt endoderm specification or morphogenesis, such as *casanova* (*cas*; *sox32* – ZFIN) and *miles apart* (*mil*; *edg5* – ZFIN), result in cardia bifida. The *cas* locus encodes a Sox-related transcription factor that is required cell-autonomously for endoderm specification (Alexander et al., 1999; Dickmeis et al., 2001; Kikuchi et al., 2001). The *mil* locus encodes a sphingosine-1-phosphate receptor that plays a cell non-autonomous role in recruiting cardiomyocytes to the midline (Kupperman et al., 2000). Endoderm morphogenesis is disrupted in *mil* mutants (Kupperman et al., 2000), possibly as a consequence of defects in endoderm-extracellular matrix interactions (Matsui et al., 2007), and the *mil* myocardial defects are presumed to be a result of the observed endoderm defects. We tracked cardiomyocytes in both *cas* mutants and *mil* mutants. As we observed comparable phenotypes in both cases, we focus here on our *mil* mutant data.

Examination of cardiomyocyte movements in *mil* mutants revealed a lack of initial medial movement, followed by a later phase of regionally restricted angular movement (Fig. 3A-G and see Movie 3 in the supplementary material). Although *mil* mutant cardiomyocytes remained stationary for most of the time period that encompasses wild-type cardiac fusion, the mutant cells initiated movement by the 20-somite stage. At this time, anterior and posterior cardiomyocytes exhibited striking angular movements (Fig. 3C-G and Table 1). Once this movement had begun, the mean rate of *mil* mutant cardiomyocyte movement (0.29±0.18 μm/minute) was similar to the mean rate observed during the second phase of wild-type cardiac fusion (0.36±0.03 μm/minute). Central cardiomyocytes typically exhibited no net directed movement over the course of the time-lapse (16 of 18 cells observed in *mil* mutants; Fig. 3C,D and Table 1). Continuation of this pattern of movement results in the formation of two lateral cardiac cones that extend into independent tubes (data not shown) (Yelon et al., 1999). Thus, the *mil* mutant phenotype indicates that the angular movements that establish the cardiac cone can occur even in the absence of initial medial movement.

Endocardium actively induces cardiomyocyte movement

Our data indicate that cone formation in cardia bifida mutants involves angular cell movements reminiscent of those observed during wild-type cone formation (Fig. 3C-G and Fig. 1G,H,L,M), suggesting that

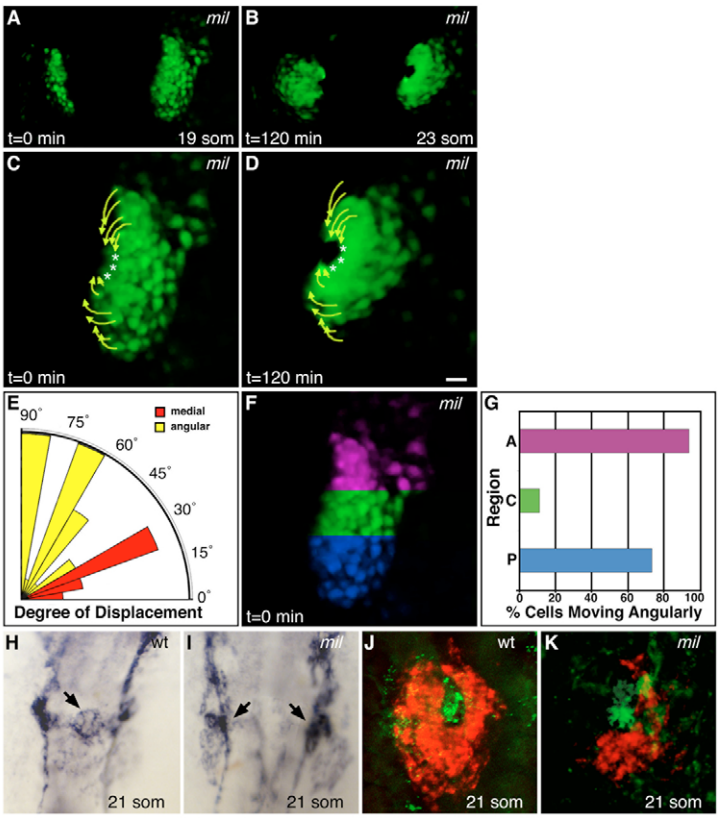

Fig. 3. Angular cell movement occurs in the absence of initial medial movement. (**A-D**) Selected images from a time-lapse of cardiac fusion in a typical *mil* mutant zebrafish embryo expressing *Tg(cmlc2:egfp)* (see Movie 3 in the supplementary material), exhibiting cardiac morphology at the (A) 19-somite and (B) 23-somite stages. Dorsal views, anterior to the top. (C,D) Paths traveled by cardiomyocytes in the right lateral heart field during the entire time-lapse (arrows and asterisks as described for Fig. 1). Tracks displayed represent a subset of the tracked cells in this time-lapse. Although initial medial movement is lost, *mil* mutant cardiomyocytes exhibit a phase of angular movement. Images in C,D are double the magnification of those in A,B. Scale bar: 20 μm. (**E**) Radial bar graph (see Fig. 1J,L) depicting degree of displacement for all tracked *mil* mutant cardiomyocytes. Most cells exhibit angular movement. (**F**,**G**) Location of cardiomyocytes moving angularly in *mil* mutants. In *mil* mutants, as in wild-type embryos, angular movement is regionally restricted. See Table 1 for additional data. (**H**,**I**) In situ hybridization for *flk1* (*kdr* – ZFIN) expression in wild-type (H) and *mil* mutant (I) embryos at the 21-somite stage. Dorsal views, anterior to the top; both images shown at the same magnification. Arrows indicate clusters of presumed endocardial precursors. (**J**,**K**) Two-color fluorescent in situ hybridization for expression of *cmlc2* (red) and *fli1a* (green) in wild-type (J) and *mil* mutant (K) embryos at the 21-somite stage. Dorsal views, anterior to the top; only the right lateral heart field is shown in K; both images shown at the same magnification. In both wild-type and *mil* mutant embryos, the presumed endocardial precursors are clustered adjacent to the central cardiomyocytes.

lateral cone formation might also depend on the presence of endocardium. In *mil* mutants, the presumed endocardial precursors do not move to the midline (Fig. 3H-K). Instead, these cells remained clustered laterally, adjacent to the central regions of the *mil* mutant heart fields (Fig. 3H-K). Thus, angular cardiomyocyte movements are directed toward centrally located endocardial cells in both wild-type and *mil* mutant embryos. To test whether endocardium is required for the angular movements observed in *mil* mutants, we tracked cardiomyocyte movements in *mil;clo* double mutants (Fig. 4A-D and see Movie 4 in the supplementary material). *mil;clo* double mutants displayed the expected lateral heart fields; however, unlike *mil* mutant cardiomyocytes, *mil;clo* double-mutant cardiomyocytes did not display any directed movement (Fig. 4C,D). Although cells appeared to jostle relative to their neighbors, they did not exhibit net medial or angular movement. As a consequence, the *mil;clo* double mutants did not form cardiac cones or tubes; instead, each heart field remained as a sheet of cells. Thus, the *mil;clo* double-mutant phenotype, like the *clo* mutant phenotype, suggests that the endocardium is required for angular cardiomyocyte movement during cone formation. Moreover, the requirement for endocardium in a cardia bifida scenario suggests that the endocardium is not merely an obstacle that diverts the medial progress of cardiomyocyte movement. Rather, the endocardium appears to play an active role in inducing the angularly directed cell movements that configure the cardiac cone.

DISCUSSION

Differential requirements for two distinct phases of cardiac fusion

Together, our data provide a new resolution of the cellular mechanisms regulating heart tube assembly. We find that cardiac fusion involves two morphologically and genetically separable phases of directed cell movement (Fig. 5). During the first phase, coherent medial movement (Fig. 5A, red arrows) recruits cardiomyocytes toward the midline. Transition into the second phase features a significant change in the direction of movement of anterior and posterior cardiomyocytes; these angular movements (Fig. 5A, yellow arrows) integrate the contralateral populations into a properly shaped cardiac cone. These two modes of cell behavior are regulated independently: *clo* mutant cardiomyocytes undergo the first phase but do not progress into the second (Fig. 5B), whereas *mil* mutant cardiomyocytes proceed through the second phase without having experienced the first (Fig. 5C). These results suggest that the first phase of cardiac fusion, but not the second, requires myocardium-endoderm interactions (Fig. 5C), whereas the second phase of cardiac fusion, but not the first, requires myocardium-endocardium interactions (Fig. 5B,D).

Endocardium influences the induction, direction and duration of cardiomyocyte movement

Our data suggest a new function for the endocardium in regulating myocardial behavior: the endocardium actively provokes a critical transition in cardiomyocyte movement, inducing a phase of movement that is necessary to shape the cardiac cone. The endocardium may also actively dictate the angular direction of cardiomyocyte movement during the second phase of cardiac fusion. However, our data cannot rule out a more passive mechanism in which the physical position of the endocardial cells influences the angle of cardiomyocyte movement. In addition to its role in triggering cardiomyocyte movement, the endocardium also appears important for bringing cardiomyocytes to a halt: it is likely that the duration of central cardiomyocyte movement is limited by the physical impediment of the centrally located endocardial precursors.

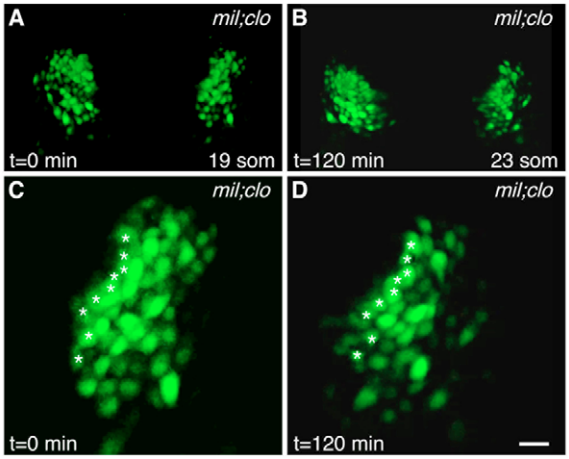

Fig. 4. Endocardium directs cardiomyocyte movement, even in the absence of initial medial movement. (**A-D**) Selected images from a time-lapse of cardiac fusion in a *mil;clo* double-mutant zebrafish embryo expressing *Tg(cmlc2:egfp)* (see Movie 4 in the supplementary material), exhibiting cardiac morphology at the (A) 19-somite and (B) 23-somite stages. Dorsal views, anterior to the top. (C,D) Paths traveled by cardiomyocytes in the right lateral heart field during the entire time-lapse (asterisks as described in Fig. 1). Images in C,D are three times the magnification of those in A,B. Scale bar: 20 μm. Example shown is representative of four heart fields analyzed. Cardiomyocytes in *mil;clo* double mutants exhibit no net directed movement.

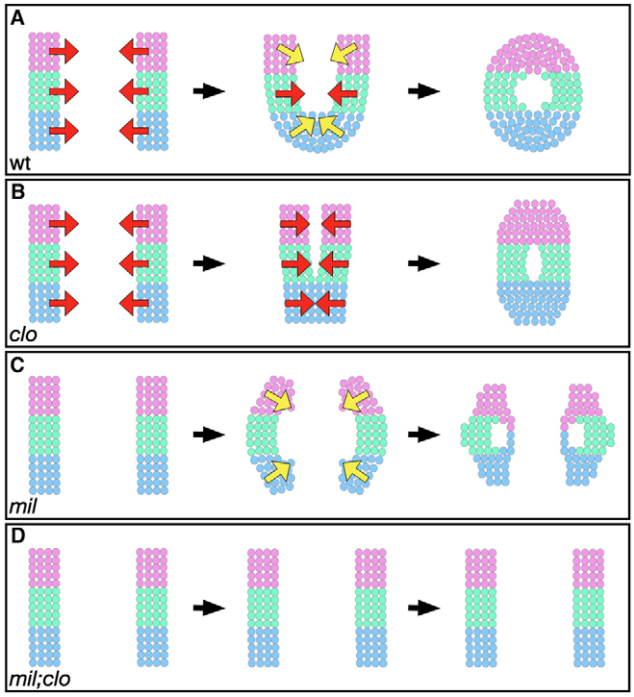

Fig. 5. Patterns of cell movement demonstrate differential requirements for two discrete phases of cardiac fusion in zebrafish. (**A**) Cardiac fusion begins with a phase of medial cardiomyocyte movement (red arrows). Cardiac cone formation is facilitated by a second phase of regionally restricted angular movement (yellow arrows). (**B**) In the absence of endocardium, as in *clo* mutants, medial movement proceeds, but angular movement is lost, resulting in a dysmorphic cardiac cone. (**C**) In cardia bifida mutants such as *mil*, medial movement is lost, but angular movement proceeds, resulting in the formation of bilateral cardiac cones. (**D**) In *mil;clo* double mutants, all cardiomyocyte movement is lost, indicating a requirement for endocardium for induction of the angular movement observed in *mil* mutants.

The molecular mechanisms by which the endocardium stimulates cardiomyocyte movement remain to be explored. The endocardium might communicate with the myocardium via direct cell-cell contacts or via secreted cues. Previous studies have demonstrated multiple requirements for myocardial-endocardial crosstalk during later phases of heart development. For example, myocardial-endocardial communication mediated by Tgf-β, Wnt, Notch, Calcineurin and Vegf signaling is crucial during atrioventricular valve formation (e.g. Armstrong and Bischoff, 2004; Beis et al., 2005; Chang et al., 2004; Hurlstone et al., 2003; Lee et al., 2006; Timmerman et al., 2004). Additionally, Neuregulin and Plexin-Semaphorin signaling are crucial during trabecular outgrowth (Meyer et al., 1997; Toyofuku et al., 2004), Neuregulin and Notch signaling are crucial during specification of the cardiac conduction system (Milan et al., 2006; Rentschler et al., 2002), and Heart of glass signaling is crucial during chamber wall thickening (Mably et al., 2003). In future work, it will be interesting to evaluate whether any of these signaling pathways are crucial for the myocardial-endocardial interactions that coordinate heart tube assembly. Alternatively, endocardium could play a less direct role, perhaps contributing to the local deposition of extracellular matrix components (Trinh and Stainier, 2004) in a way that affects the available routes for cardiomyocyte movement.

The regulation of cardiomyocyte behavior by the endocardium reveals a dynamic cellular mechanism by which two populations interact to create the foundation for an embryonic organ. By directing cardiomyocyte movement during cone formation, the endocardium establishes key parameters of heart tube morphology. We speculate that the importance of myocardial-endocardial interactions during heart tube assembly might be broadly conserved, even though the specific geometry of tube formation varies between species (Glickman and Yelon, 2002; Harvey, 2002; Moorman and Christoffels, 2003). In this regard, it is interesting to compare our findings with data regarding cardiac morphogenesis in *Ciona intestinalis* (Davidson et al., 2005). The *Ciona* embryo contains a pair of cardiac progenitor cells that exhibit two separate phases of directed movement as they travel from their origin in the tail toward the ventral midline. First, the cardiac progenitor cells migrate anteriorly in close association with the endoderm. Then, the cells switch direction and move ventrally to facilitate cardiac fusion at the midline. Combining data from zebrafish and *Ciona*, we suggest that a two-phase model of cardiac fusion might be applicable throughout chordate phyla, with an initial phase of cardiomyocyte recruitment relying on interactions with the endoderm, and a second phase of cardiomyocyte integration relying on independent factors such as those supplied by the endocardium during zebrafish cardiac cone formation.

We thank members of the Yelon laboratory, Schier laboratory and Skirball Developmental Genetics Program for helpful discussions. This work was supported by an American Heart Association Heritage Affiliate Postdoctoral Fellowship (N.G.H.) and by grants from the National Institutes of Health and American Heart Association (D.Y.). J.J.S. received support from the NYU Graduate Training Program in Developmental Genetics (NIH T32 HD007520).

Supplementary material

Supplementary material for this article is available at
http://dev.biologists.org/cgi/content/full/134/12/2379/DC1

References

Alexander, J., Rothenberg, M., Henry, G. L. and Stainier, D. Y. R. (1999). *casanova* plays an early and essential role in endoderm formation in zebrafish. *Dev. Biol.* **215**, 343-357.

Armstrong, E. J. and Bischoff, J. (2004). Heart valve development: endothelial cell signaling and differentiation. *Circ. Res.* **95**, 459-470.

Beis, D., Bartman, T., Jin, S. W., Scott, I. C., D'Amico, L. A., Ober, E. A., Verkade, H., Frantsve, J., Field, H. A., Wehman, A. et al. (2005). Genetic and cellular analyses of zebrafish atrioventricular cushion and valve development. *Development* **132**, 4193-4204.

Chang, C. P., Neilson, J. R., Bayle, J. H., Gestwicki, J. E., Kuo, A., Stankunas, K., Graef, I. A. and Crabtree, G. R. (2004). A field of myocardial-endocardial NFAT signaling underlies heart valve morphogenesis. *Cell* **118**, 649-663.

Chen, J. N., Haffter, P., Odenthal, J., Vogelsang, E., Brand, M., Van Eeden, F. J. M., Furutani-Seiki, M., Granato, M., Hammerschmidt, M., Heisenberg, C. P. et al. (1996). Mutations affecting the cardiovascular system and other internal organs in zebrafish. *Development* **123**, 293-302.

Davidson, B., Shi, W. and Levine, M. (2005). Uncoupling heart cell specification and migration in the simple chordate Ciona intestinalis. *Development* **132**, 4811-4818.

Dehaan, R. L. (1963). Migration patterns of the precardiac mesoderm in the early chick embryo. *Exp. Cell Res.* **29**, 544-560.

Dickmeis, T., Mourrain, P., Saint-Etienne, L., Fischer, N., Aanstad, P., Clark, M., Strähle, U. and Rosa, F. (2001). A crucial component of the endoderm formation pathway, CASANOVA, is encoded by a novel sox-related gene. *Genes Dev.* **15**, 1487-1492.

Glickman, N. S. and Yelon, D. (2002). Cardiac development in zebrafish: coordination of form and function. *Semin. Cell Dev. Biol.* **13**, 507-513.

Harvey, R. P. (2002). Patterning the vertebrate heart. *Nat. Rev. Genet.* **3**, 544-556.

Huang, C. J., Tu, C. T., Hsiao, C. D., Hsieh, F. J. and Tsai, H. J. (2003). Germ-line transmission of a myocardium-specific GFP transgene reveals critical regulatory elements in the cardiac myosin light chain 2 promoter of zebrafish. *Dev. Dyn.* **228**, 30-40.

Hurlstone, A. F., Haramis, A. P., Wienholds, E., Begthel, H., Korving, J., Van Eeden, F., Cuppen, E., Zivkovic, D., Plasterk, R. H. and Clevers, H. (2003). The Wnt/beta-catenin pathway regulates cardiac valve formation. *Nature* **425**, 633-637.

Keegan, B. R., Meyer, D. and Yelon, D. (2004). Organization of cardiac chamber progenitors in the zebrafish blastula. *Development* **131**, 3081-3091.

Kikuchi, Y., Agathon, A., Alexander, J., Thisse, C., Waldron, S., Yelon, D., Thisse, B. and Stainier, D. Y. (2001). *casanova* encodes a novel Sox-related protein necessary and sufficient for early endoderm formation in zebrafish. *Genes Dev.* **15**, 1493-1505.

Kupperman, E., An, S., Osborne, N., Waldron, S. and Stainier, D. Y. (2000). A sphingosine-1-phosphate receptor regulates cell migration during vertebrate heart development. *Nature* **406**, 192-195.

Lee, Y. M., Cope, J. J., Ackermann, G. E., Goishi, K., Armstrong, E. J., Paw, B. H. and Bischoff, J. (2006). Vascular endothelial growth factor receptor signaling is required for cardiac valve formation in zebrafish. *Dev. Dyn.* **235**, 29-37.

Li, S., Zhou, D., Lu, M. M. and Morrisey, E. E. (2004). Advanced cardiac morphogenesis does not require heart tube fusion. *Science* **305**, 1619-1622.

Liao, W., Bisgrove, B., Sawyer, H., Hug, B., Bell, B., Peters, K., Grunwald, D. and Stainier, D. (1997). The zebrafish gene *cloche* acts upstream of a *flk-1* homologue to regulate endothelial cell differentiation. *Development* **124**, 381-389.

Lyons, I., Parsons, L. M., Hartley, L., Li, R., Andrews, J. E., Robb, L. and Harvey, R. P. (1995). Myogenic and morphogenetic defects in the heart tubes of murine embryos lacking the homeo box gene *Nkx2-5*. *Genes Dev.* **9**, 1654-1666.

Mably, J. D., Mohideen, M. A., Burns, C. G., Chen, J. N. and Fishman, M. C. (2003). *heart of glass* regulates the concentric growth of the heart in zebrafish. *Curr. Biol.* **13**, 2138-2147.

Matsui, T., Raya, A., Callol-Massot, C., Kawakami, Y., Oishi, I., Rodriguez-Esteban, C. and Belmonte, J. C. (2007). *miles-apart*-mediated regulation of cell-fibronectin interaction and myocardial migration in zebrafish. *Nat. Clin. Pract. Cardiovasc. Med.* **4** Suppl. 1, S77-S82.

Meyer, D., Yamaii, T., Garratt, A., Riethmacher-Sonnenberg, E., Kane, D., Theill, L. E. and Birchmeier, C. (1997). Isoform-specific expression and function of neuregulin. *Development* **124**, 3575-3586.

Milan, D. J., Giokas, A. C., Serluca, F. C., Peterson, R. T. and MacRae, C. A. (2006). Notch1b and neuregulin are required for specification of central cardiac conduction tissue. *Development* **133**, 1125-1132.

Moorman, A. F. and Christoffels, V. M. (2003). Cardiac chamber formation: development, genes, and evolution. *Physiol. Rev.* **83**, 1223-1267.

Narita, N., Bielinska, M. and Wilson, D. B. (1997). Wild-type endoderm abrogates the ventral developmental defects associated with GATA-4 deficiency in the mouse. *Dev. Biol.* **189**, 270-274.

O'Brien, T. X., Lee, K. J. and Chien, K. R. (1993). Positional specification of ventricular myosin light chain 2 expression in the primitive murine heart tube. *Proc. Natl. Acad. Sci. USA* **90**, 5157-5161.

Qian, F., Zhen, F., Ong, C., Jin, S. W., Meng Soo, H., Stainier, D. Y., Lin, S., Peng, J. and Wen, Z. (2005). Microarray analysis of zebrafish *cloche* mutant using amplified cDNA and identification of potential downstream target genes. *Dev. Dyn.* **233**, 1163-1172.

Rentschler, S., Zander, J., Meyers, K., France, D., Levine, R., Porter, G., Rivkees, S. A., Morley, G. E. and Fishman, G. I. (2002). Neuregulin-1 promotes formation of the murine cardiac conduction system. *Proc. Natl. Acad. Sci. USA* **99**, 10464-10469.

Stainier, D. Y. R., Lee, R. K. and Fishman, M. C. (1993). Cardiovascular development in the zebrafish. I. Myocardial fate map and heart tube formation. *Development* **119**, 31-40.

Stainier, D. Y. R., Welnstein, B. M., Detrich, H. W., Zon, L. I. and Fishman, M. C. (1995). *cloche*, an early acting zebrafish gene, is required by both the endothelial and hematopoietic lineages. *Development* **121**, 3141-3150.

Stalsberg, H. and DeHaan, R. L. (1969). The precardiac areas and formation of the tubular heart in the chick embryo. *Dev. Biol.* **19**, 128-159.

Thompson, M., Ransom, D., Pratt, S., MacLennan, H., Kieran, M., Detrich, H. W., Vail, B., Huber, T., Paw, B., Brownlie, A. et al. (1998). The *cloche* and *spadetail* genes differentially affect hematopoiesis and vasculogenesis. *Dev. Biol.* **197**, 248-269.

Timmerman, L. A., Grego-Bessa, J., Raya, A., Bertran, E., Perez-Pomares, J. M., Diez, J., Aranda, S., Palomo, S., McCormick, F., Izpisua-Belmonte, J. C. et al. (2004). Notch promotes epithelial-mesenchymal transition during cardiac development and oncogenic transformation. *Genes Dev.* **18**, 99-115.

Toyofuku, T., Zhang, H., Kumanogoh, A., Takegahara, N., Yabuki, M., Harada, K., Hori, M. and Kikutani, H. (2004). Guidance of myocardial patterning in cardiac development by Sema6D reverse signalling. *Nat. Cell Biol.* **6**, 1204-1211.

Trinh, L. A. and Stainier, D. Y. (2004). Fibronectin regulates epithelial organization during myocardial migration in zebrafish. *Dev. Cell* **6**, 371-382.

Yelon, D., Horne, S. A. and Stainier, D. Y. R. (1999). Restricted expression of cardiac myosin genes reveals regulated aspects of heart tube assembly in zebrafish. *Dev. Biol.* **214**, 23-37.